Acta Crystallographica Section A
Foundations of Crystallography
ISSN 0108-7673

Received 15 September 2004
Accepted 11 October 2004

Three-beam diffraction in an elastically strained crystal plate

Helge B. Larsen,[a]* Gunnar Thorkildsen[b] and Edgar Weckert[c]

[a]Department of Materials Science, University of Stavanger, N-4068 Stavanger, Norway, [b]Department of Mathematics and Natural Science, University of Stavanger, N-4068 Stavanger, Norway, and [c]HASYLAB at DESY, Notkestrasse 85, D-22607 Hamburg, Germany. Correspondence e-mail: helge.b.larsen@tn.his.no

Based on the Takagi–Taupin equations, an analytical expression for the three-beam diffraction profile function in an elastically strained crystal plate is derived. The strain parameters appear in the shape functions governing both triplet-phase dependent and independent terms in the solution. Simulations show that three-beam profiles are significantly influenced. With increasing strain any phase information in the profiles is obscured and subsequently lost.

1. Introduction

A three-beam diffraction case arises when a secondary lattice node is gradually excited on to the Ewald sphere by *e.g.* rotating the crystal around a primary reciprocal-lattice vector **h**, fulfilling Bragg's law. For a perfect crystal plate, the self-consistent balance of the excited wave amplitudes, leading to observable interference effects, is very well described within the framework of the so-called fundamental equations of X-ray dynamical diffraction theory (Colella, 1974; Authier, 2001).

In the late 70s and the early 80s, it was experimentally shown that such effects were visible in imperfect (or 'mosaic') crystals too (Post, 1977; Chapman *et al.*, 1981; Chang, 1982; Thorkildsen & Mo, 1982). However, the subsequent theoretical developments were still aimed at clarifying various aspects of the diffraction physics in perfect crystals – see for instance the review article by Weckert & Hümmer (1997). The influence of crystal imperfection (in its broadest sense) has not undergone any extensive theoretical investigations in the literature. Normally, mosaicity (along with instrumental broadening) has been accounted for by a convolution of the intrinsic diffraction profile with a smearing function modelled either as a Lorentzian (Chang & Tang, 1988; Shen *et al.*, 2000) or as a Gaussian (Weckert & Hümmer, 1997); consult also Thorkildsen *et al.* (2003). In all these cases, the distribution functions are *ad hoc* taken into account at a rather late stage in the analysis.

Another interesting development is due to Kohn and co-workers who used three-beam diffraction concepts to obtain a depth profile of crystal distortion (Kohn, 1988; Kohn & Samoilova, 1992). This has been further extended by Schroer (1998), who, by numerical simulations, included effects of strain owing to multilayer deposition. Among other applications of three-beam diffraction in non-perfect crystals, one should mention the determination of lattice mismatch in thin layered materials outlined by Chang (1984) and the determination of piezoelectric constants by Avanci *et al.* (1998, 2000). A different approach, directly addressing the issue of crystal imperfection, has been devised by the present authors, who applied the principles of statistical dynamical theory to account for the propagation of the coherently scattered waves from randomly distorted samples (Larsen & Thorkildsen, 1998*b*).

In the following, we include a displacement field of the imperfection state in question – elastic strain – at the beginning of the analysis. This is straightforwardly done within the Takagi–Taupin formalism. We will consider a semi-infinite crystal plate (no lateral boundaries) and perform an analysis similar to that described in our previous paper (Thorkildsen *et al.*, 2001), hereafter denoted TLW. The solution is analytical, expressed as a series expansion with a finite number of terms, including the one carrying the information about the invariant-phase triplet as well as phase-independent terms representing *Aufhellung* and *Umweganregung*. The result applies to thin plates, as discussed in TLW.

2. Theory

2.1. Governing equations

A convenient way to include a gentle deformation field, $\mathbf{u}(\mathbf{r})$, associated with the imperfection state of the crystal, is inherent in the Takagi–Taupin equations (Takagi, 1962, 1969; Taupin, 1964). These have been extensively applied in the two-beam case [consult Authier (2001) for a comprehensive review] to model diffraction from distorted crystals. The formalism, in its perfect-crystal limit, has also been developed for three-beam diffraction in finite samples (Thorkildsen, 1987; Thorkildsen & Larsen, 1998).

The Takagi–Taupin equations for one state of polarization may generally be written in terms of the amplitudes of the

constituent waves, p, of the electrical displacement field (optical field):

$$\frac{\partial D_p}{\partial s_p} = 2\pi i \beta'_p D_p + i \sum_{q \neq p} \kappa_{pq} D_q. \quad (1)$$

For the three-beam case, $p, q \in \{o, h, g\}$, where o designates the incoming beam, while h and g refer to the primary diffracted and the secondary diffracted beam, respectively. Scattering among the beams is brought about by the lattice planes with associated reciprocal-lattice vectors $\pm\mathbf{h}$, $\pm\mathbf{g}$ and $\pm(\mathbf{h} - \mathbf{g})$. For a uniformly deformed crystal, *cf.* Authier (2001), equation (14.2*b*),[1]

$$\beta'_p = \beta_p - \frac{\partial}{\partial s_p}[\mathbf{p} \cdot \mathbf{u}(\mathbf{r})], \quad p \in \{h, g\}. \quad (2)$$

β_o is put equal to zero. Provided the deformation field (see below) is of such a character that the deviation parameters $\{\beta'_p\}$ are constant in space, the unitary transformation, $D_p = \tilde{D}_p \exp(2\pi i \sum_q \beta'_q s_q)$, yields

$$\frac{\partial \tilde{D}_p}{\partial s_p} = i \sum_{q \neq p} \kappa_{pq} \tilde{D}_q. \quad (3)$$

One should notice that in the derivation of the Takagi–Taupin equations only first-order terms are retained, while those $\propto |\nabla^2(\mathbf{p} \cdot \mathbf{u})|$ are neglected (Takagi, 1969). This puts limits on the deformation fields that might actually be analyzed by the present approach. Implicitly, polarization coupling effects are not considered. In addition, in accordance with TLW, neither ordinary absorption nor refraction (Larsen & Thorkildsen, 1998*a*) are included. The coordinate s_p is along the wavevector $\mathbf{K}_p$ associated with the diffracted beam and $\hat{\mathbf{s}}_p$ the corresponding unit vector. $\mathbf{r}$ is a real-space position vector. The coupling coefficient, κ_{pq}, is given by

$$\kappa_{pq} = (\lambda r_e / V_c) F_{pq} C_{pq},$$

where r_e is the classical electron radius, V_c is the unit-cell volume, λ the wavelength, F_{pq} the structure factor associated with the reciprocal-lattice node $p - q$ and C_{pq} is the polarization factor for σ or π polarization. It represents the scattering power per unit length for a plane wave propagating with wavevector $\mathbf{K}_q$ fulfilling the diffraction condition for the reciprocal-lattice vector $\mathbf{p} - \mathbf{q}$. The deviation parameter β_p (Authier *et al.*, 1968) is set equal to the excitation error, α_p, associated with the reflection p. From an experimentalist's point of view, this implies a parametrization by the rocking angle of the primary reflection as $\alpha_h \propto \Delta\omega$, and the azimuthal rotation angle about the primary lattice vector as $\alpha_g \propto \Delta\psi$. As we focus on the integrated power of the primary diffracted beam, $\Delta\psi$ will govern the simulated three-beam diffraction profile as discussed in TLW.

2.2. Deformation field

We consider a simple deformation field: elastic strain. The following model is adopted:

$$\mathbf{u}(\mathbf{r}) = \mathbf{u}(s_h, s_g) = \varepsilon_h s_h \hat{\mathbf{s}}_h + \varepsilon_g s_g \hat{\mathbf{s}}_g, \quad (4)$$

where $\varepsilon_{h,g}$ signifies strain components in the $\hat{\mathbf{s}}_h$ and $\hat{\mathbf{s}}_g$ direction, respectively. For the special geometrical case considered, fully symmetrical Laue–Laue diffraction with $\angle(\hat{\mathbf{s}}_p, \hat{\mathbf{s}}_q) = 2\theta_{pq} = 2\theta$, the deviation parameters become

$$\beta'_{h,g} = \alpha_{h,g} - (2\sin^2\theta/\lambda)\varepsilon_{h,g}. \quad (5)$$

2.3. Principle of solution

The principle of solution is accounted for in detail in TLW, but for the sake of completeness some major points are repeated here. The crystal plate and corresponding diffraction geometry are depicted in Fig. 1. We consider a point source located at S. The electrical displacement field associated with the primary diffracted beam at the point P on the exit surface is

$$D_h(P \leftarrow S) \propto \tilde{D}_h(\Delta_o, \Delta_h, \Delta_g) \exp(2\pi i \beta'_h \Delta_h) \exp(2\pi i \beta'_g \Delta_g),$$

where $\Delta_p = s_p(P) - s_p(S)$. $\tilde{D}_h$ is the boundary-value Green function, associated with equation (3), for the primary diffracted wavefield. In order to obtain the field at the exit point P, the amplitude contributions from all source points within the base abc of the inverted Borrmann pyramid have to be summed. That is,

$$D_h(P) = D_h(P \mid \beta'_h, \beta'_g) \propto \iint_{abc} \mathrm{d}A_S \, D_h(P \leftarrow S),$$

where $\mathrm{d}A_S$ is an area element of the entrance surface. The Green function is expressed as a series expansion,

$$\tilde{D}_h(\Delta_o, \Delta_h, \Delta_g) = D_o^{(e)} \sum_{j=1}^{\infty} d_h^{(j)}(\Delta_o, \Delta_h, \Delta_g),$$

where $D_o^{(e)}$ is the source amplitude. Owing to the increasing complexity, it is not worthwhile here to consider terms of order higher than 3. Hence,

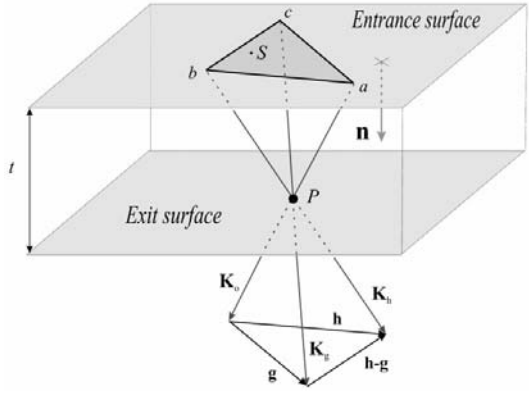

Figure 1
Crystal and scattering geometry. Symmetrical Laue–Laue diffraction. Slab thickness t. The scattering volume giving the displacement field at exit point P is the inverted Borrmann pyramid $abcP$. The origin of the (s_o, s_h, s_g) coordinate system is also located at P. The wavevectors $\mathbf{K}_o$, $\mathbf{K}_h$ and $\mathbf{K}_g$ all form an angle γ with the inward-drawn normal vector $\hat{\mathbf{n}}$.

[1] In this work, β'_p is not scaled to the wavenumber, thus its dimension is Å^{-1}.

$$d_h^{(1)} = \delta(\Delta_g),$$
$$d_h^{(2)} = \frac{\lambda r_e}{V_c}\frac{|F_{hg}||F_{go}|}{|F_{ho}|}\frac{C_{hg}C_{go}}{C_{ho}}(i\cos\Phi_\Sigma - \sin\Phi_\Sigma),$$
$$d_h^{(3)} = -\Delta_o\Delta_h\kappa_{oh}\kappa_{ho}\delta(\Delta_g) - \Delta_o\kappa_{og}\kappa_{go} - \Delta_h\kappa_{hg}\kappa_{gh}.$$

$\Phi_\Sigma = \phi_{oh} + \phi_{hg} + \phi_{go}$ is the structure-invariant triplet phase sum and $\delta(\,)$ represents the Dirac δ function. The remaining steps in the calculation consist of determining the diffracted power distribution and the integrated power. For a semi-infinite crystal plate, the power is independent of the choice of reference point P on the exit surface. Thus the integrated power is given by

$$\mathcal{P}_h \propto \int_{-\infty}^{\infty} \mathrm{d}\Delta\omega\, |D_h(P|\beta'_h, \beta'_g)|^2.$$

In this integration, terms of type

$$\int_{-\infty}^{\infty} \mathrm{d}x\, \{\sin x \sin(x - x_1)/[x(x - x_2)^m(x - x_3)^n]\}, \qquad m, n \in \{0, 1, 2\}$$

are interpreted as Cauchy principal values.

3. Results and discussion

The result for the integrated power is

$$\mathcal{P}_h = \mathcal{P}_h^{(0)}\Big\{1 - \tfrac{1}{3}\eta_{oh}^2 - 2\frac{\eta_{hg}\eta_{go}}{\eta_{ho}} \times [f_1(\zeta_g, \zeta_h)\sin\Phi_\Sigma + f_2(\zeta_g, \zeta_h)\cos\Phi_\Sigma] - 2[\eta_{go}^2 f_{A1}(\zeta_g, \zeta_h) + \eta_{hg}^2 f_{A2}(\zeta_g, \zeta_h)] + 2\frac{\eta_{hg}^2\eta_{go}^2}{\eta_{ho}^2} f_U(\zeta_g)\Big\}. \quad (6)$$

Here $\mathcal{P}_h^{(0)}$ is the kinematical integrated power, and we have defined the following dimensionless quantities, *cf.* equations (7) and (8) of TLW:

$$\eta_{pq} = (t/\cos\gamma)(\lambda r_e/V_c)|F_{pq}|C_{pq} \quad (7a)$$
$$\zeta_g = (2\pi t/\cos\gamma)\alpha_g - \zeta_0\varepsilon_g = \xi_g - \zeta_0\varepsilon_g, \quad (7b)$$
$$\zeta_h = \zeta_0\varepsilon_h, \quad (7c)$$
$$\zeta_0 = (4\pi t\sin^2\theta/\lambda\cos\gamma). \quad (7d)$$

The extended shape functions are given by

$$f_1(\zeta_g, \zeta_h) = \frac{\zeta_h - \zeta_g - \zeta_h\cos\zeta_g + \zeta_g\cos\zeta_h}{\zeta_h\zeta_g^2 - \zeta_h^2\zeta_g},$$
$$f_2(\zeta_g, \zeta_h) = \frac{\zeta_g\sin\zeta_h - \zeta_h\sin\zeta_g}{\zeta_h\zeta_g^2 - \zeta_h^2\zeta_g},$$
$$f_{A1}(\zeta_g, \zeta_h) = \frac{\zeta_h[\zeta_g(\zeta_g - \zeta_h) + \zeta_h\sin\zeta_g] - \zeta_g^2\sin\zeta_h}{\zeta_h^2(\zeta_h - \zeta_g)\zeta_g^2},$$
$$f_{A2}(\zeta_g, \zeta_h) = \frac{\zeta_h\zeta_g(\zeta_g - \zeta_h)\cos\zeta_h - \zeta_h^2\sin\zeta_g + (2\zeta_h - \zeta_g)\zeta_g\sin\zeta_h}{\zeta_h^2(\zeta_h - \zeta_g)^2\zeta_g},$$
$$f_U(\zeta_g) = \frac{\zeta_g - \sin\zeta_g}{\zeta_g^3}. \quad (8)$$

These functions should be compared with the perfect crystal results, TLW equations (6)–(11). We observe that the strain parameters are included in the independent variables of the shape functions. Furthermore, in the perfect-crystal limit,

$$\lim_{\varepsilon_h,\varepsilon_g\to 0} f_1(\zeta_g, \zeta_h) = (1 - \cos\xi_g)/\xi_g^2,$$
$$\lim_{\varepsilon_h,\varepsilon_g\to 0} f_2(\zeta_g, \zeta_h) = (\xi_g - \sin\xi_g)/\xi_g^2,$$
$$\lim_{\varepsilon_h,\varepsilon_g\to 0} f_{A1}(\zeta_g, \zeta_h) = \lim_{\varepsilon_h,\varepsilon_g\to 0} f_{A2}(\zeta_g, \zeta_h) = f_U(\xi_g),$$

the correct values are retrieved. Thus the expression for the integrated power becomes identical to the one published for the perfect crystal plate [equation (6) in TLW]. It is interesting to note that the introduction of this specific strain field gives different shape functions, f_{A1} and f_{A2}, for the two *Aufhellung* terms, *cf.* Fig. 2. This is in contrast to the perfect-crystal limit, where both these terms, as well as the *Umweganregung* term, are governed by the same (one-dimensional) shape function (f_3 in TLW, which is identical to f_U). The *Aufhellung* terms have their origin in interference between a single scattered wave through the coupling κ_{ho} and the triple scattered ones, caused by the couplings $\kappa_{ho}\kappa_{og}\kappa_{go}$ and $\kappa_{hg}\kappa_{gh}\kappa_{ho}$, respectively. These two cases of multiple reflections will occur along different optical routes (Kato, 1976) and in a strained crystal they will not experience the same lattice deformations. We also note that *Umweganregung*, as it appears in our model, is invariant of the strain parameter ζ_h.

In order to exemplify the findings, we now consider the complete symmetrical Laue–Laue case $2\bar{2}0/0\bar{2}2/20\bar{2}$ in silicon. The expression for the relative change of the integrated power owing to three-beam diffraction effects may then be expressed by (the extinction correction term is omitted)

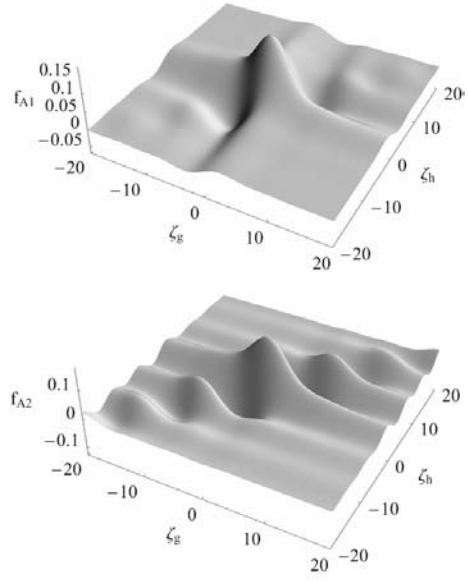

Figure 2
Three-dimensional plots of the shape functions associated with the *Aufhellung* terms.

$$\frac{\Delta\mathcal{P}_h(\zeta_g,\zeta_h)}{\mathcal{P}_h^{(0)}} = -2\Bigg\{\eta_0\frac{C_{hg}C_{go}}{C_{ho}}[f_1(\zeta_g,\zeta_h)\sin\Phi_\Sigma + f_2(\zeta_g,\zeta_h)\cos\Phi_\Sigma] + \eta_0^2\Bigg[C_{go}^2 f_{A1}(\zeta_g,\zeta_h) + C_{hg}^2 f_{A2}(\zeta_g,\zeta_h) - \left(\frac{C_{hg}C_{go}}{C_{ho}}\right)^2 f_U(\zeta_g)\Bigg]\Bigg\}. \quad (9)$$

The dimensionless variables ζ_g and ζ_h are expressed in 'experimental terms' by parameterizing

$$\zeta_g = (a\Delta\psi - b\,\varepsilon_g)t, \quad \zeta_h = b\varepsilon_h t.$$

Relevant numerical values for the parameters relating to the actual scattering situation in silicon are given in Table 1, consult also §3 of TLW.

A finite value of ε_g causes a shift in the zero point of the three-beam profile, given by

$$\Delta\psi^{(0)} \approx 1.8\varepsilon_g.$$

This is also reported in the literature, *e.g.* Fig. 5 of Avanci *et al.* (1998). Otherwise, this strain parameter will not influence the shape of the three-beam profile.

In Fig. 3, three-beam profiles for various crystal strains, ε_h, are presented. Following the discussion in TLW, the series-expansion approach is valid for the crystal thickness $t = 2$ µm used in the simulations. We observe that crystal strain strongly influences the shape of the three-beam diffraction profiles. A correct phase interpretation is obscured already at $\varepsilon_h \sim 0.0002$. Here, the triplet phase sum seems to be changed by approximately 90°. Such an apparent phase change has also been predicted in strained layer systems by numerical simulations (Schroer, 1998). Any phase information vanishes completely at about $\varepsilon_h \sim 0.001$, and the interference effects fade away as the strain, *i.e.* imperfection, increases. The strain values are within the fracture limit of silicon, for which the typical fracture strain varies between ∼0.004 and ∼0.007 (Brantley, 1973; Yi *et al.*, 2000). The plots show significant influence of small changes in the strain, which also indicates the feasibility of three-beam diffraction as a sensitive tool for measuring the effects of minute structural changes in the scattering system.

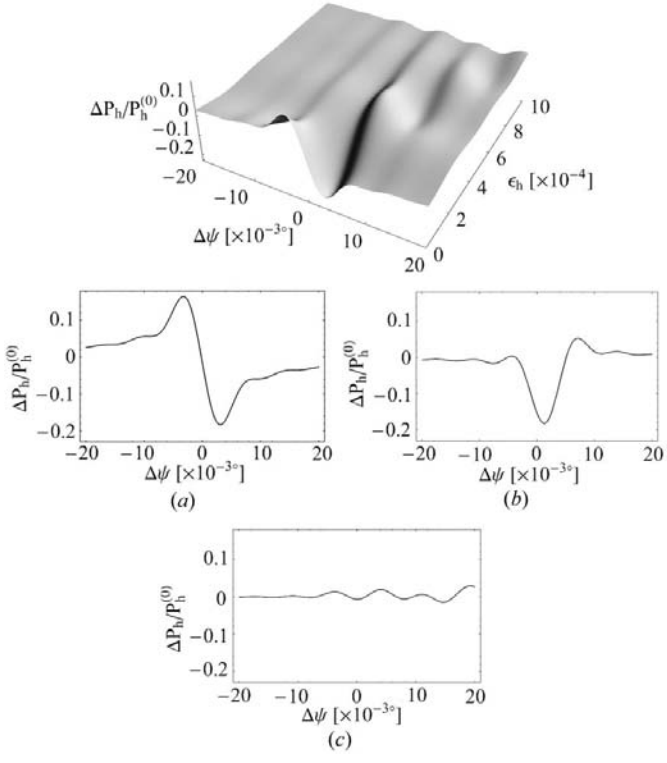

Figure 3
Influence of crystal strain, ε_h, on three-beam diffraction profiles $2\bar{2}0/0\bar{2}2/20\bar{2}$, in a silicon crystal plate of thickness 2 µm. $\varepsilon_g = 0$. Parameters as given in Table 1. Three-dimensional presentation and selected profiles: (*a*) perfect-crystal case ($\varepsilon_h = 0$); (*b*) $\varepsilon_h = 0.0002$; (*c*) $\varepsilon_h = 0.0010$. $\Delta\psi < 0$ corresponds to the situation when **g** is inside the Ewald sphere.

Table 1
Parameters relevant for the model calculations.

π polarization is assumed and the polarization factors are calculated according to Weckert & Hümmer (1997). $\Delta\psi$ is measured in units of 10^{-3}°, t in micrometres, λ in Å and $\varepsilon_{h,g}$ in units of 10^{-4}. Using these conventions, a and b are presented as dimensionless quantities.

$\hat{\mathbf{n}}$	λ	t	a	b	η_0	Φ_Σ	C_{oh}	$C_{og} = C_{hg}$
$\bar{1}\bar{1}\bar{1}$	1.000	2.0	0.4947	0.8935	0.2535	0.0	0.8644	−0.9655

4. Concluding remarks

It is shown theoretically that crystal imperfection significantly alters the three-beam diffraction profiles. For the simple deformation field considered in the present analysis, small elastic distortions tend to change the asymmetry of the profile. If strain is increased, interference effects completely vanish and any 'dynamical' information is subsequently lost. Such behavior is generally to be expected as the perfection state of the crystal is changed when strain is introduced.

A model for elastic strain including terms quadratic in the coordinates, *e.g.* $s_p s_q$ (Katagawa & Kato, 1974; Chukhovskii & Petrashen, 1977), has been extensively studied in the two-beam case – consult chapters 13 and 14 of Authier (2001) for further details. However, for the three-beam case, it still remains a serious challenge to develop an analytical treatment, at least within the present series-expansion approach, for more complex cases than the one presented here. An extension to deformation fields not linear in the spatial coordinates calls for a generalized unitary transformation of type $D_p \rightarrow \tilde{D}_p \exp[2\pi i \sum_q \int_0^{s_q} \mathrm{d}s'_q\,\beta'_q]$ in order to obtain an expression equivalent to equation (3). Another possibility for considering other and more realistic strain fields is to apply numerical techniques. Proper algorithms for solving the Takagi–Taupin equations for the three-beam case are then a prerequisite. The work of Schroer (1998) should in this context provide an excellent starting point.

References

Authier, A. (2001). *Dynamical Theory of X-ray Diffraction.* Oxford: Oxford Science Publications.

Authier, A., Malgrange, C. & Tournarie, M. (1968). *Acta Cryst.* A**24**, 126–136.

Avanci, L., Cardoso, L., Girdwood, S., Pugh, D. & Sherwood, J. (1998). *Phys. Rev. Lett.* **81**, 5426–5429.

Avanci, L., Cardoso, L., Sasaki, J., Girdwood, S., Roberts, K., Pugh, D. & Sherwood, J. (2000). *Phys. Rev. B*, **61**, 6507–6514.

Brantley, W. A. (1973). *J. Appl. Phys.* **44**, 534–535.

Chang, S.-L. (1982). *Phys. Rev. Lett.* **48**, 163–166.

Chang, S.-L. (1984). *Multiple Diffraction of X-rays in Crystals.* Berlin: Springer Verlag.

Chang, S.-L. & Tang, M.-T. (1988). *Acta Cryst.* A**44**, 1065–1072.

Chapman, L. D., Yoder, D. R. & Colella, R. (1981). *Phys. Rev. Lett.* **46**, 1578–1581.

Chukhovskii, F. & Petrashen, P. (1977). *Acta Cryst.* A**33**, 311–319.

Colella, R. (1974). *Acta Cryst.* A**30**, 413–423.

Katagawa, T. & Kato, N. (1974). *Acta Cryst.* A**30**, 830–836.

Kato, N. (1976). *Acta Cryst.* A**32**, 453–457.

Kohn, V. G. (1988). *Phys. Status Solidi A*, **106**, 31–37.

Kohn, V. G. & Samoilova, L. V. (1992). *Phys. Status Solidi A*, **133**, 9–16.

Larsen, H. B. & Thorkildsen, G. (1998*a*). *Acta Cryst.* A**54**, 129–136.

Larsen, H. B. & Thorkildsen, G. (1998*b*). *Acta Cryst.* A**54**, 137–145.

Post, B. (1977). *Phys. Rev. Lett.* **39**, 760–763.

Schroer, K. (1998). *Phasenempfindliche Röntgenbeugung an Oberflächen und Schichtsystemen.* PhD thesis, Universität Karlsruhe (TH), Karlsruhe, Germany.

Shen, Q., Kycia, S. & Dobrianov, I. (2000). *Acta Cryst.* A**56**, 268–279.

Takagi, S. (1962). *Acta Cryst.* **15**, 1311–1312.

Takagi, S. (1969). *J. Phys. Soc. Jpn*, **26**, 1239–1253.

Taupin, D. (1964). *Bull. Soc. Fr. Minéral. Cristallogr.* **87**, 469–511.

Thorkildsen, G. (1987). *Acta Cryst.* A**43**, 361–369.

Thorkildsen, G. & Larsen, H. B. (1998). *Acta Cryst.* A**54**, 120–128.

Thorkildsen, G., Larsen, H. B. & Weckert, E. (2001). *Acta Cryst.* A**57**, 389–394.

Thorkildsen, G., Larsen, H. B., Weckert, E. & Semmingsen, D. (2003). *J. Appl. Cryst.* **36**, 1324–1333.

Thorkildsen, G. & Mo, F. (1982). Abstracts of the 7th European Crystallographic Meeting, Jerusalem, Israel, p. 6.

Weckert, E. & Hümmer, K. (1997). *Acta Cryst.* A**53**, 108–143.

Yi, T., Li, L. & Kim, C.-J. (2000). *Sensors Actuators*, **83**, 172–178.